23rd ABCM International Congress of Mechanical Engineering
December 6-11, 2015, Rio de Janeiro, RJ, Brazil

FERROFLUID DROPLET HEATING AND VAPORIZATION UNDER HIGH MAGNETIC POWER: A SPHERICAL GEOMETRY MODEL

R. Zorzo
C. F. C. Cristaldo
Universidade Federal do Pampa
regis10z@gmail.com, cesarcristaldo@unipampa.edu.br

F. F. Fachini
Instituto Nacional de Pesquisas Espaciais
fachini@lcp.inpe.br

Abstract.
The models of heating and vaporization of ferrofluid fuel droplet under the influence of external magnetic fields has been recently studied. This process is known as relaxation magnetic heating. The magnetic heating within the droplet together with heat transfer provided from the gaseous environment are responsible to accelerate the ferrofluid fuel droplet. When exposed to an external alternating magnetic field, the nanoparticles dissipate heat through both Brownian and Néel relaxations within the droplet. In the Brownian relaxation the nanoparticle rotate together with its dipole generating heat by friction between nanoparticle and surrounding fluid. In the Néel relaxation the dipole rotate with the nanoparticle fixed, consequently the nanoparticle is heated by "internal friction" due to the movement of the magnetic moment within the nanoparticle. Under a certain frequency of the alternating magnetic field, the droplet core is rapidly heated. Thus the magnetic heating increase the vaporization rate and consequently produce a combustion with less emission of pollutants. The present model is an extension of previous works in which the condition of large magnetic power is considered. A thermal boundary layer is established within the droplet close to the surface. In the present model the solution is obtained in spherical geometry in order to compare with a thermal boundary layer model described by a planar geometry. The results show that there are a small difference between the two model. The thermal boundary layer solution present underestimated results such as vaporization rate, temperature surface of the droplet and heating time is greater than the present model.

Keywords: *combustion, droplet, nanofluid, ferrofluid*

1. INTRODUCTION

Nanofluid fuels, a new class of nanotechnology-based fuels, are fuels with a stable suspension of nanometer-sized particles. The properties and behavior of a nanofluid fuel depend on a number of parameters including the properties of the fuel, nanoparticle concentration, nanoparticle size and morphology, as well as the presence of dispersant and/or surfactant that is responsible to maintaining the homogeneous distribution of nanoparticles in the fluid. Many studies have been conducted in the field of heating, vaporization and combustion of the nanofluid fuels Plantier *et al.* (2005); Mitchell *et al.* (2008); Tyagi *et al.* (2008); Yetter *et al.* (2009); Selvan *et al.* (2009); Chen *et al.* (2010); Oronzio and Yogesh (2010). The nanoparticles significantly change properties of the fluid, such as thermal conductivity, viscosity and specific heat. These changes in properties result in desirable effects on combustion, such as decrease in ignition delay, increase of the heat transfer, reduction of the pollutant emissions. Previous studies shown a 20% increase in the thermal conductivity of ethanol containing 4% volume fraction of aluminum nitrate nanoparticles. In other study, in the aerosol shock tube, the addition of 2% (by weight) Al nanoparticles in ethanol and $JP-8$ can reduce their ignition delays by 32% and 50%, respectively (Gan *et al.*, 2012). Nanoparticles affect the time scale of chemical reactions, contributing to decrease of ignition delay time (A. Pivkina, 2004). In addition, the surface tension of a liquid fuel can be reduced depending on the type and concentration of nanoparticle and surfactant, favoring its vaporization (Tanvir and Qiao, 2012; Gerken *et al.*, 2014). Nanoparticles can be used as additive in diesel and diesel-biodiesel-ethanol blend to improve complete combustion of the fuel and reduce the exhaust emissions (Selvan *et al.*, 2009). More specific studies reveal a complex chair mechanisms that can occur during the burning of fuel droplets, for example, the burn of a specific nanofluid fuel droplet can present distinctive stages: preheating, ignition, classical combustion, microexplosion, surfactant flame, and nanoparticle droplet flame and possible nanoparticle scape from the surface of the droplet to the gas-phase (Gan, 2011; Gan *et al.*, 2012).

Recently, magnetic nanoparticles has been used in fuels, ferrofluid fuels (Taylor *et al.*, 2013). The advantages of ferrofluid over nanofluid is that the flow and transport processes of energy can be controlled by adjusting an external magnetic field, besides the changes in fluid properties. Experimental tests shown that the effects of adding water-based ferrofluid to diesel fuel improve the engine performance and changes the exhaust emission characteristics of the fuel, such as NO_x emissions decrease and CO emissions increase. After the combustion, the magnetic nanoparticles can be collected by magnetic bar (Shafii *et al.*, 2011).

The ferrofluid fuel under the application of external magnetic field has been studied recently. Since the diameter of the suspended magnetic particles is usually about 10 nm, these nanoparticles are considered to have a single magnetic moment (Xuan, 2000). Ferrofluid when exposed to an alternating magnetic field can generate heat due to rotation of the nanoparticles within the fluid or due the magnetic moment rotations inside the nanoparticles (Rosensweig, 2002). This heating process is known as magnetic heating and recently, has been applied in the combustion field.

In the first work, the vaporization of an isolated ferrofluid droplet fuel was studied whereas that the droplet at its boiling temperature is exposed to magnetic heating process. The results show that the heating time is reduced by the application of alternating magnetic fields (Fachini and Bakuzis, 2010). In later works, the transient heating process of the liquid phase was included in the model and different conditions were studied: heating and vaporization at different ambient temperatures and Lewis number different to unity (Cristaldo and Fachini, 2013a; Cristaldo *et al.*, 2015). In other work, the combustion problem was included in the model (Cristaldo and Fachini, 2013b). The result shown that the flame position, vaporization rate, and flame temperature can be controlled by the frequency of magnetic field. All these works consider the condition of very large magnetic power, as a result a thermal boundary layer is established close to its surface in the liquid side. Thus the solution is obtained by a boundary layer solution model, named BLS model. In the BLS model, the solution is obtained in appropriate spatial and time scales by a change of variables. As a consequence, the solution loses the spherical geometry of the physical problem.

The present analysis aims to solve the same physical problem in spherical geometry, in order to evaluate the effect of geometry on the numerical solution of the problem under the condition of large magnetic power. This model will be named as complete solution (CS model).

2. FORMULATION

Fuel droplet with uniform distribution of magnetic nanoparticles within is considered. The droplet is placed in a quiescent environment so that it has spherical symmetry. Under the application of an external magnetic field, the droplet is heated by magnetic relaxation mechanism. With decreasing particle size the energy barrier for magnetization reversal decrease, too, and consequently thermal fluctuations lead to two relaxation mechanisms, Néel and Brownian (Maenosono and Saita, 2006; Hergt *et al.*, 2006).

The Néel relaxation mechanism occurs by magnetic dipole rotation inside the droplet without rotation of the particle. The Brownian relaxation mechanism occurs through particle rotation in the liquid. In the Néel mechanism, the fluctuation of the magnetic moment direction across an anisotropy barrier, the characteristic relaxation time of a nanoparticle system is given by the ratio of the anisotropy energy $\overline{K}V_H$ to thermal energy κT^*, thus the Néel relaxation time is defined by $t_N^* = t_o exp\left(\overline{K}V_H/\kappa T^*\right)$, in which $\overline{K}$ (J/m^3) is the anisotropy constant, V_H the hydrodynamic volume, t_o the characteristic time which is typically assumed to be 10^{-9} s and $\kappa = 1.38 \times 10^{-23}$ J/K is Boltzmann's constant, T^* is temperature.

In the fluid characterized by a viscosity η, the Brownian relaxation mechanism is given by $t_B^* = 3\eta V_n/\kappa T^*$, in which η is the viscosity of the liquid and V_n is the nanoparticle volume. Generally, heating power is dominated by the faster regime of relaxation, resulting in an effective relaxation time $1/t_e^* = 1/t_N^* + 1/t_B^*$. In the present work, the Brownian mechanism is dominant under high magnetic frequencies that is the condition addressed in this analysis.

The droplet is assumed to be spherical with radius $a(t)$ at time t, $a_0 = a(0)$ being the initial value. It is assumed that the density ρ, the specific heat of the liquid phase c_l and thermal conductivity of the liquid phase k_l are constant. The presence of nanoparticles within the droplet results in changes of these properties, but in the present analysis it will not be considered. The dimensionless variables used in this work are defined as:

$$t \equiv t^*/t_c, \quad r \equiv r^*/\bar{a}_0, \quad \theta \equiv T^*/T_B^*, \quad \rho \equiv \rho^*/\rho_\infty^*, \quad u \equiv u^* a^*(0)/\alpha_\infty, \quad a \equiv a^*/a^*(0) \tag{1}$$

in which t, r, ρ, θ, u and a represent time, relaxation time, radial coordinate, density, temperature, gas velocity and droplet radius, respectively. The characteristic time is defined by the droplet heating time $t_c = [a_0^2/(k_g/c_p\rho_\infty)](\rho_l/\rho_\infty)$, T_B^* is the boiling temperature, k_g the thermal conductivity of the fuel vapor, c_p the specific heat of the fuel vapor, ρ_l and ρ_∞ are density of the liquid and gas phases. The equation for mass and energy dimensionless conservation, (Fachini, 1999a), are given by

$$\frac{d}{dt}(a^3) = -3\lambda(t) \tag{2}$$

$$\frac{\partial\theta}{\partial t} - \frac{A}{r^2}\frac{\partial\theta}{\partial r}\left(r^2\frac{\partial\theta}{\partial r}\right) = P_m\frac{f^2 t_e(\theta)}{[f t_e(\theta)]^2+1} \tag{3}$$

in which $\lambda(t) \equiv \dot{m}(t^*)c_p/(4\pi k_g a^*(0))$ is the dimensionless vaporization rate, $A = c_p k_l/c_l k_g$, $f = 2\pi\bar{f}t^*_{e_b}$ is the dimensionless frequency, $t_e(\theta) = t^*_e/t_{e_b}$ is the dimensionless relaxation time that is a function of temperature, in which the subscript b states the boiling condition. Thus the magnetic power is defined by

$$P_m = \frac{\mu_0\chi_0 H_0^2/2}{\rho_l c_l T_B}\frac{t_c}{t^*_{e_b}} \tag{4}$$

in which μ_0 is the magnetic permeability, χ_0 the magnetic field amplitude and H_0^2. The dimensionless parameter P_m represents the ratio of the power magnetic to the thermal power due to the heat conduction from the gas phase. The present work considers the case $P_m >> 1$. This means that the power magnetic is the very large compared to the thermal power. Equation 3 and the following boundary conditions:

$$\left.\frac{\partial\theta}{\partial r}\right|_{x=0} = 0 \tag{5}$$

in the droplet core, and

$$a^2\theta^n\left.\frac{\partial\theta}{\partial r}\right|_{a^+} = Aa^2\left.\frac{\partial\theta}{\partial r}\right|_{r=a^-} + \lambda L \tag{6}$$

in the droplet surface describe the evolution of the temperature profile inside the droplet. The latent heating of vaporization L^* in dimensionless form is defined by $L = L^*/(c_p T^*)$.

In the gas-phase, the conservation equations are presented below Fachini (1999a,b):

$$\epsilon\frac{\partial\rho}{\partial\tau} + \frac{1}{r^2}\frac{\partial}{\partial r}(r^2\rho u) = 0, \tag{7}$$

$$\epsilon\rho\frac{\partial Y_F}{\partial\tau} + \rho u\frac{\partial Y}{\partial r} - \frac{1}{r^2}\frac{\partial}{\partial r}\left(\frac{r^2\theta^n}{L_F}\frac{\partial Y_F}{\partial r}\right) = 0, \tag{8}$$

$$\epsilon\rho\frac{\partial\theta}{\partial\tau} + \rho u\frac{\partial\theta}{\partial r} - \frac{1}{r^2}\frac{\partial}{\partial r}\left(r^2\theta^n\frac{\partial\theta}{\partial r}\right) = 0, \tag{9}$$

in which Y_F is the vapor mass fraction of the fuel and L_F is the vapor Lewis number of the fuel. Under condition of low pressure $\epsilon \equiv \rho_\infty/\rho_l$, the gas phase processes can be treated as quasi-steady-state. Thus the conservation equations can be rewritten as

$$r^2\rho u = \lambda(t), \tag{10}$$

$$\frac{\lambda(t)}{r^2}\frac{\partial Y_F}{\partial r} - \frac{1}{r^2}\frac{\partial}{\partial r}\left(\frac{r^2\theta^n}{L_F}\frac{\partial Y_F}{\partial r}\right) = 0, \tag{11}$$

$$\frac{\lambda(t)}{r^2}\frac{\partial\theta}{\partial r} - \frac{1}{r^2}\frac{\partial}{\partial r}\left(r^2\theta^n\frac{\partial\theta}{\partial r}\right) = 0. \tag{12}$$

The boundary conditions at the surface are described by Eq.(6) and

$$-\frac{r^2\theta^n}{Le}\frac{\partial Y_F}{\partial r} = \lambda(1 - Y_{F_s}), \quad \text{at} \quad r = a^+. \tag{13}$$

the vapor mass fraction at the surface is given by $Y_{F_s} = exp[\gamma(1 - \theta_b/\theta_s]$, where $\gamma \equiv L^* M_w/(R_g T^*_b)$, in which M_w is the liquid molecular weight M_w and R_g is the universal gas constant.

In the region far from the droplet, the following boundary conditions hold

$$\theta = \theta_\infty, \quad \text{and} \quad Y_F = 0 \quad \text{at} \quad r \to \infty. \tag{14}$$

Equations (11) and (12) can be integrated once considering the boundary conditions given by Eqs. (13), (14) and the energy conservation at the interface, Eq.(6), resulting in the following system

$$\frac{\partial\theta}{\partial r} = \frac{\lambda(t)(\theta - \theta_s + L) + Q^-}{r^2\theta^n}, \tag{15}$$

$$\frac{\partial Y_F}{\partial r} = -\frac{\lambda(t)(1 - Y_F)L_F}{r^2\theta^n}, \tag{16}$$

in which $Q^- \equiv Aa^2(\partial\theta/\partial r)_{r=a^-}$ is the heat flux from surface to inner region of the droplet. The numerical solutions of Eqs.(15, 16 are obtained by shooting method of integration, the numerical procedure can be chosen in previous work (Cristaldo and Fachini, 2013a).

3. Results

The results of magnetic heating n-heptane fuel droplet are presented. The droplet is placed in quiescent atmosphere at 2200K (six times the boiling temperature). This temperature was chosen in order to reproduce qualitatively the flame temperature. The fuel Lewis number is considered equal to unity. The properties of n-heptane, gas-phase, nanoparticles and gas phase are shown in the table 1, 2

Table 1. Constants properties

liquid phase		gas phase	
ρ_l	1100 g/m^3	ρ_l	680640 g/m^3
c_g	1 $J/(g.K)$	c_l	2.2359 $J/(g.K)$
k_g	0.025 $J/(m.s.K)$	k_l	316.76 $J/(m.s.K)$
T_b^*	371 K	T_∞^*	2200 K
L^*	329.57 J/g		

Table 2. nanoparticles and magnetic field constant properties

nanoparticles		magnetic field	
a_0	10^{-9} m	Md	425000 A/m
ϕ	0.07	B_o	0.7 T

The present model, named as complete solution (CS), is compared to previous model Cristaldo and Fachini (2013a), named boundary layer solution (BLS). In both models the condition of very large magnetic power, $P_m >> 1$, is considered. Under this condition, a thermal boundary layer is established in the liquid phase, close to the droplet surface.

Figure 1 shows the droplet radius square as a function of the time for both models, CS and BLS. The linear decrease of the droplet radius square is observed in the classical models of droplet heating and vaporization (without magnetic heating). In the present model, the linear decrease is not observed because the heating occurs simultaneously with the vaporization. In addition can be observed that the heating occurs in a short time resulting in little reduction of the radius, thus the linear decrease of the droplet square could only be observed after droplet to reach its boiling temperature, condition not addressed in both models.

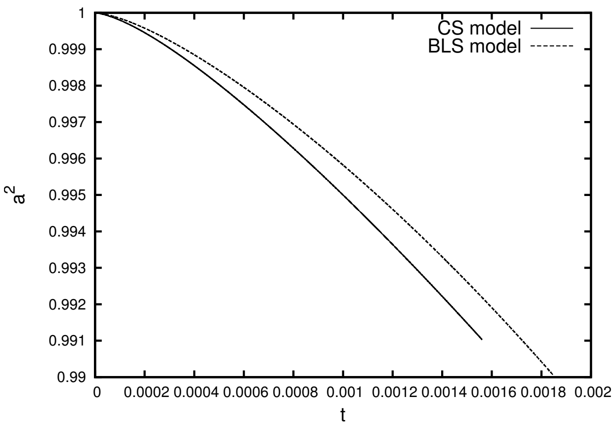

Figure 1. Droplet radius square as a function of time

Figure 2 shows the temperature of the droplet surface as a function of the time determined by two models. The temperature of the droplet surface is underestimated by BLS model. Thus the geometric effect is important for conditions imposed by the problem ($P_m = 100$). Moreover, the temporal evolution of the droplet temperature at the center is identical in both models. This shows that the geometric effect is more important in the droplet surface. The BLS model having a lower surface temperature compared to the CS model, it is expected that the rate of vaporization is underestimated, as shown Fig.4.

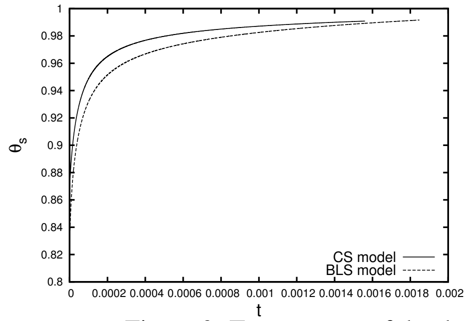

Figure 2. Temperature of the droplet surface as a function of time

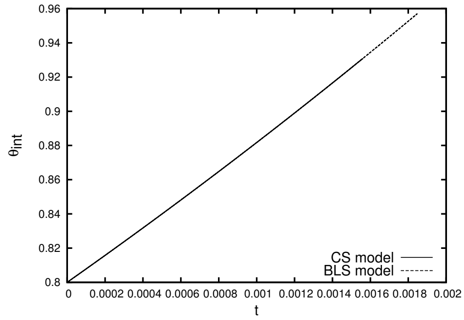

Figure 3. Temperature of the droplet core as a function of time

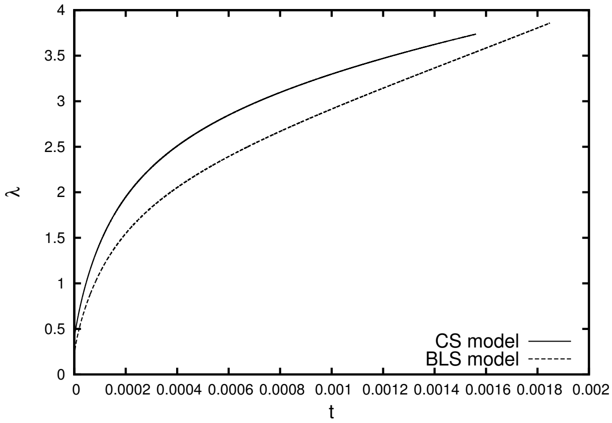

Figure 4. Vaporization rate as a function of time

4. CONCLUSION

The magnetic heating of the ferrofluid fuel droplet placed in an environment of high temperature is studied. The solution in spherical geometry, CS model, is obtained and compared to thermal boundary layer solution, BLS , in planar geometry under condition of large magnetic power. The result shows that the loss of spherical geometry by thermal boundary layer solution is considerable under condition of $P_m = 100$. This shows that the BLS model would be best represented by parameter $P_m > 1$. In addition, the present model can be used to condition of $P_m = O(1)$, condition not valid to BLS model. This condition is more realistic and can be used to evaluate the energy cost.

A. Pivkina, P. Ulyanova, Y.F.S.Z.J.S., 2004. "Nanomaterials for heterogeneous combustion". *Propellants, Explosives, Pyrotechnics*, Vol. 29, p. 39.

Chen, R.H., Phuoc, T.X. and Martello, D., 2010. "Effects of nanoparticles on nanofluid droplet evaporation". *International Journal of Heat and Mass Transfer*, Vol. 53, p. 3677.

Cristaldo, C.F.C. and Fachini, F.F., 2013a. "Ferrofluid droplet heating and vaporization under very large magnetic power: A thermal boundary layer model". *Physics of Fluids*, Vol. 25, p. 037101.

Cristaldo, C.F. and Fachini, F.F., 2013b. "Analysis of ferrofluid droplet combustion under very large magnetic power". *Combustion and Flame*, Vol. 160, p. 1458.

Cristaldo, C.F., Vargas, M.M. and Fachini, F.F., 2015. "Ferrofluid droplet vaporization under very large magnetic power: Effects of pressure and effective thermal conductivity of liquid". *Proceedings of the Combustion Institute*, Vol. 35, p. 1613.

Fachini, F.F., 1999a. "An Analytical Solution for the Quasi-Steady Droplet Combustion". *Combustion and Flame*, Vol. 306, p. 302.

Fachini, F.F. and Bakuzis, a.F., 2010. "Decreasing nanofluid droplet heating time with alternating magnetic fields". *Journal of Applied Physics*, Vol. 108, p. 084309.

Fachini, F. F., W.F.A., 1999b. "Theory of Flame Histories in Droplet Combustion at Small Stoichiometric Fuel-Air Ratios". *AIAA Journal*, Vol. 37, p. 1426.

Gan, Yanan, Q.L., 2011. "Evaporation characteristics of fuel droplets with the addition of nanoparticles under natural and forced convections". *International Journal of Heat and Mass Transfer*, Vol. 54, p. 4913.

Gan, Y., Lim, Y.S. and Qiao, L., 2012. "Combustion of nanofluid fuels with the addition of boron and iron particles at dilute and dense concentrations". *Combustion and Flame*, Vol. 159, p. 1732.

Gerken, W.J., Thomas, A.V., Koratkar, N. and Oehlschlaeger, M.a., 2014. “Nanofluid pendant droplet evaporation: Experiments and modeling”. *International Journal of Heat and Mass Transfer*, Vol. 74, p. 263.

Hergt, R., Dutz, S., Müller, R. and Zeisberger, M., 2006. “Magnetic particle hyperthermia: nanoparticle magnetism and materials development for cancer therapy”. *Journal of Physics: Condensed Matter*, Vol. 18, p. S2919.

Maenosono, S. and Saita, S., 2006. “Theoretical assessment of FePt nanoparticles as heating elements for magnetic hyperthermia”. *Magnetics, IEEE Transactions on*, Vol. 42, p. 1638.

Mitchell, M.R., Link, R.E., Kao, M.J., Ting, C.C., Lin, B.F. and Tsung, T.T., 2008. “Aqueous Aluminum Nanofluid Combustion in Diesel Fuel”. *Journal of Testing and Evaluation*, Vol. 36, p. 100579.

Oronzio, M. and Yogesh, J., 2010. “Heat Transfer in Nanofluids”. Vol. 2010.

Plantier, K.B., Pantoya, M.L. and Gash, A.E., 2005. “Combustion wave speeds of nanocomposite Al/Fe2O3: the effects of Fe2O3 particle synthesis technique”. *Combustion and Flame*, Vol. 140, p. 299.

Rosensweig, R., 2002. “Heating magnetic fluid with alternating magnetic field”. *Journal of Magnetism and Magnetic Materials*, Vol. 252, p. 370.

Selvan, V., Anand, R. and Udayakumar, M., 2009. “Effects of cerium oxide nanoparticle addition in diesel and diesel-biodiesel-ethanol blends on the performance and emission characteristics of a CI engine”. *Journal of Engineering and Applied Sciences*, Vol. 4, p. 1.

Shafii, M.B., Daneshvar, F., Jahani, N. and Mobini, K., 2011. “Effect of Ferrofluid on the Performance and Emission Patterns of a Four-Stroke Diesel Engine”. *Advances in Mechanical Engineering*, Vol. 2011, p. 1.

Tanvir, S. and Qiao, L., 2012. “Surface tension of nanofluid-type fuels containing suspended nanomaterials”. *Nanoscale research letters*, Vol. 7, p. 226.

Taylor, R., Coulombe, S., Otanicar, T., Phelan, P., Gunawan, A., Lv, W., Rosengarten, G., Prasher, R. and Tyagi, H., 2013. “Small particles, big impacts: A review of the diverse applications of nanofluids”. *Journal of Applied Physics*, Vol. 113, p. 011301.

Tyagi, H., Phelan, P.E., Prasher, R., Peck, R., Lee, T., Pacheco, J.R. and Arentzen, P., 2008. “Increased hot-plate ignition probability for nanoparticle-laden diesel fuel”. *Nano letters*, Vol. 8, p. 1410.

Xuan, Y., 2000. “Heat transfer enhancement of nanofluids”. *International Journal of Heat and Fluid Flow*, Vol. 21, p. 58.

Yetter, R.A., Risha, G.A. and Son, S.F., 2009. “Metal particle combustion and nanotechnology”. *Proceedings of the Combustion Institute*, Vol. 32, p. 1819.

5. RESPONSIBILITY NOTICE

The authors are the only responsible for the printed material included in this paper.